Broadband semiconductor superlattice detector for THz radiation

F. Klappenberger, A. A. Ignatov,[a] S. Winnerl,[b] E. Schomburg, W. Wegscheider, and K. F. Renk[c]
Institut für Angewandte Physik, Universität Regensburg, 93040 Regensburg, Germany

M. Bichler
Walter-Schottky-Institute München, 85748 Garching, Germany

(Received 18 September 2000; accepted for publication 8 January 2001)

We report on a broadband GaAs/AlAs superlattice detector for THz radiation; a THz field reduces the current through a superlattice, which is carried by miniband electrons, due to modulation of the Bloch oscillations of the miniband electrons. We studied the detector response, by use of a free electron laser, in a large frequency range (5–12 THz). The responsivity showed strong minima at frequencies of infrared active phonons of the superlattice. A theoretical analysis of the detector delivers an understanding of the role of phonons and gives a characterization of the responsivity.
 [DOI: 10.1063/1.1352669]

In experiments with superlattices showing negative differential conductance due to Bloch oscillations, it has been reported[1–3] that THz irradiation of a current carrying GaAs/AlAs superlattice lead to a reduction of the current through the superlattice; detection of radiation has been demonstrated up to 5 THz. In this letter we show that the superlattice detector, operated at room temperature, can be applied in a wide frequency range extending beyond 10 THz, and that the responsivity has minima at the frequencies of infrared active phonons. We compare the actual responsivity with the theoretical upper limit for superlattice detectors on the basis of Bloch oscillations.

A superlattice (superlattice A) was grown by molecular beam epitaxy on a (100) oriented semi-isolating GaAs substrate and consisted of 100 periods of 14 monolayers GaAs and 3 monolayers AlAs. It was homogeneously doped with silicon ($8\times10^{16}\,\mathrm{cm}^{-3}$) and was embedded in doped graded layers and 300 nm thick n^+ GaAs layers (doping $2\times10^{18}\,\mathrm{cm}^{-3}$). By photolithography and reactive ion etching we prepared small-area (1 μm diam) and large-area mesas and evaporated AuGeNi, forming ohmic contacts after a temperature treatment. From the offset ($\approx$1 eV) between the GaAs and AlAs conduction bands and the thicknesses of the GaAs well and AlAs barriers, we estimated the width (70 meV) of the lowest miniband and the gap (415 meV) to the next higher miniband. Transport occurred mainly by the electrons in the lowest miniband. A voltage applied across a small- and a large-area mesa in series, which were electrically connected by the n^+ GaAs layer on the substrate, was almost the voltage across the small-area mesa. For more details of sample characterization see Ref. 2.

THz radiation was coupled to the (small-area) superlattice via an antenna system [Fig. 1(a)] consisting of an AuNi wire formed to an L antenna near a 90° corner cube reflector designed for optimum acceptance of radiation around 5 THz (wavelength $\lambda=60\,\mu$m, antenna length 4 λ, distance from the apex of the reflector 1.2 λ). The superlattice was connected to a voltage source delivering a static voltage U_s. Current pulses produced by THz pulses were coupled via a capacitor to a sampling oscilloscope (time resolution 20 ps).

As the radiation source we used the free-electron laser (FELIX) in Nieuwegein, the Netherlands, delivering macropulse trains (duration 5 μs, repetition rate 5 Hz) and micropulses (repetition rate 25 MHz, duration 6 ps, pulse power 0.1–10 kW). The radiation was focused on the detector by an off-axis parabolic mirror.

The current–voltage characteristic of a superlattice [points in Fig. 1(b)] shows ohmic behavior for small voltage and a current peak (peak–current density $\approx100\,\mathrm{kA/cm}^2$) at a critical voltage (0.7 V), where a negative differential conductance sets in; in the range of negative differential conductance the current shows steps because of formation of domains along the superlattice axis. For detection, we operated the superlattice at the critical voltage, where the responsivity was largest. The signal (Fig. 2, inset) had a duration (30 ps) that was determined by the monitoring electronic circuit; for the laser power we used (pulse energy 2 nJ) there was almost

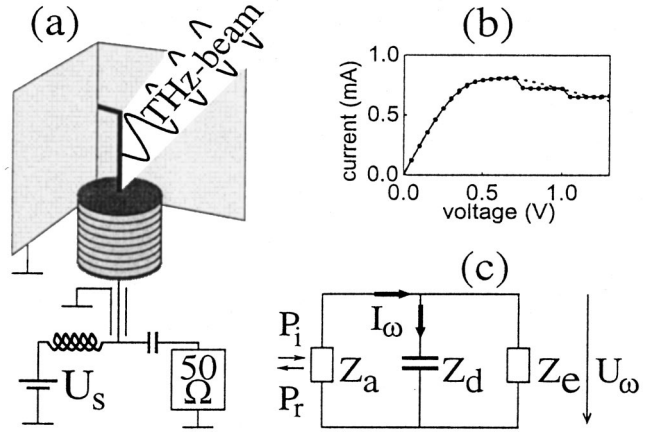

FIG. 1. Superlattice detector: (a) setup, (b) current–voltage characteristic, (c) equivalent circuit for the THz current.

[a]Permanent address: Institute for Physics of Microstructures, Russian Academy of Science, 603600 Nizhny Novgorod, Russia.
[b]Permanent address: Forschungszentrum Jülich, D-52425 Jülich, Germany.
[c]Author to whom correspondence should be addressed; electronic mail: karl.renk@physik.uni-regensburg.de

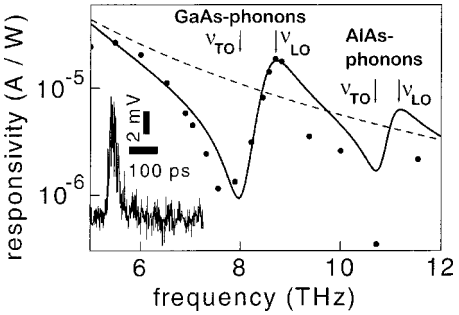

FIG. 2. Responsivity of a superlattice detector and signal pulse (inset).

no thermal heating of the superlattice as indicated by the lack of a background signal. We measured the signal height for different frequencies ν of the THz radiation and extracted the experimental responsivity $R_{ex}=\tau_{osc}/\tau_L\,(U_m/Z_{osc})P_i^{-1}$, where U_m is the voltage of the signal maximum, Z_{osc} $(=50\,\Omega)$ is the input impedance of the oscilloscope, P_i is the power of the incident radiation in the focus (diameter about 1 mm) in which the antenna was placed, τ_{osc} is the time resolution of the oscilloscope, and τ_L is the laser pulse duration.

The experimental responsivity (Fig. 2, points) shows a resonance-like behavior with a strong minimum at the infrared active transversal optic phonon frequency ν_{TO} of GaAs and a peak at the longitudinal optic phonon frequency ν_{LO}; the responsivity differs between minimum and maximum by a factor of 30. Another minimum occurs at the frequency of the infrared active phonon of AlAs. Earlier results have shown that outside the phonon resonances, at small THz frequencies, the response decreases as ν^{-4} (dashed line).

We have also studied the response for a superlattice (B) which had a larger miniband width ($\Delta\approx 140$ meV) and a larger peak–current density ($\approx 200\,\mathrm{kA/cm^2}$); we used a mesa with a diameter of 5 μm. The responsivity (Fig. 3, circles), which we measured up to 10 THz, showed again the GaAs phonon resonance, with a factor of 50 between minimum and maximum. The responsivity was about an order of magnitude larger than for superlattice A (Fig. 3, points), indicating a more efficient coupling of the THz radiation to the superlattice B. For an analysis of the experimental results, we introduce a THz current circuit [Fig. 1(c)], with the antenna impedance Z_A $(\approx 100\,\Omega)$, which we assume to be real and, in parallel to each other, the superlattice impedances Z_d and Z_e for dielectric and electron currents, respectively. We treat the case $|Z_A|\gg|Z_d|$ and assume that for THz frequencies $|Z_d|\ll|Z_e|$, i.e., that the electron THz current through the superlattice is small compared to the dielectric THz current. The incident radiation produces a THz current in the antenna I_ω, which flows mainly as dielectric current through the superlattice causing a THz voltage $U_\omega=Z_dI_\omega$ across the superlattice. Because of the mismatch between antenna and superlattice, only a small part of the incident radiation is absorbed in the superlattice, while the main part is reflected back from the antenna into the free space (P_r, reflected power). We determine the THz current by the relation $\eta P_i=\frac{1}{2}Z_A\widehat{I_\omega}^2$, where $\widehat{I_\omega}$ is the amplitude of the THz current and η an efficiency for the coupling of the free space radiation to the antenna; for a perfectly designed antenna η is near 1. The dielectric impedance of the superlattice is $Z_d=(i\omega C)^{-1}$, where $C(\omega)=\varepsilon_0\varepsilon(\omega)A/L$ is the capacity of the superlattice, ε_0 is the electric field constant, $\varepsilon(\omega)$ is the dielectric function of the superlattice, A is the cross section, and L is the length of the superlattice. It follows that $\hat{U}_\omega=(2\eta PR_A^{-1})^{1/2}L(\varepsilon_0Ai\omega\varepsilon)^{-1}$, indicating that the THz voltage amplitude is small if $|\varepsilon(\omega)|$ has a large value, which is characteristic for frequencies of infrared active phonons, and that the amplitude is large if $|\varepsilon(\omega)|$ has a small value, which is characteristic for longitudinal optic phonon frequencies.

The THz voltage produces a THz field $E_\omega=U_\omega/L$ in the superlattice which acts on the miniband electrons. We consider the motion of one electron (wave packet) and describe the interaction of the electron with both the THz field and a static field (strength $E_s=U_s/L$) by $\hbar\dot{k}=-e(E_s+\hat{E}_\omega\cos\omega t)$, where k is the center wave vector of the wave packet ($\hbar$ is Planck's constant and e is elementary charge). In the case $\hat{E}_\omega=0$ it follows for the phase $ka=\omega_Bt$, where a is the superlattice period and $\omega_B=(1/\hbar)\,ea|E_s|$ is the Bloch frequency. With the dispersion relation $\varepsilon(k)=\frac{1}{2}\Delta(1-\cos ka)$, where Δ is the miniband width, the group velocity of the electron is $v_g=(\Delta a/2\hbar)\sin(\omega_Bt+mf)$, where $m=ea(\hbar\omega)^{-1}\hat{E}_\omega$ and $f=\sin\omega t-\sin\omega t_0$, with the last term taking into account the phase between the Bloch oscillation and the THz field. The group velocity and thus the Bloch oscillation are frequency modulated with the modulation degree m. For small modulation degree ($m\ll 1$) we can expand v_g with respect to mf. The electron is submitted to intraminiband relaxation, with each relaxation process changing the phase. Averaging over all phases ($\omega t_0=0-2\pi$), we obtain for $\omega\gg\omega_B$ by time averaging and omitting all terms, which vary faster than the period of the Bloch oscillation, $v_g=(\Delta a/2\hbar)\,(1-\frac{1}{2}m^2)\sin\omega_Bt$. The electron drifts along the electric force with the drift velocity $v=(1/\tau)\int v_g\times\exp(-t/\tau)\,dt$, where τ is the intraminiband relaxation time. The integration delivers $v=(1-\frac{1}{2}m^2)v_d$, where $v_d=(1/2\hbar)\,\Delta a\,\omega_B\tau(1-\omega_B^2\tau^2)^{-1}$ is the drift-velocity-field characteristic[4] without THz field. Under the influence of a THz field the drift velocity is reduced by $\Delta v=\frac{1}{2}m^2v_d$. The strength of the direct current through the superlattice is $neAv$, where n is the carrier concentration and A the superlattice area. A THz field leads to a reduction of current, $\delta I=\frac{1}{2}m^2I$, where I is the current for $\hat{E}_\omega=0$; in Fig. 1(b) (dashed) we have shown I for our superlattice. The current reduction is proportional to m^2, i.e., the detector measures the power of the incident radiation. Maximum current reduction δI_m is obtained for $\omega_B\tau=1$. Then the responsivity is given by $R=\delta I_m/P=\frac{1}{2}m^2I_p/P$, where I_p is the peak current.

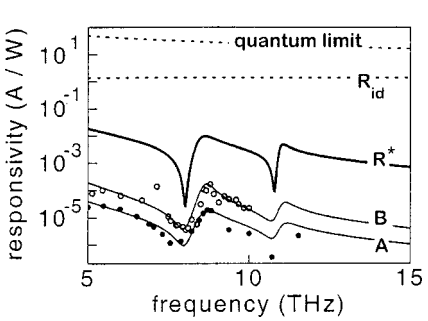

FIG. 3. Experimental and theoretical responsivity curves.

rent without THz field. The responsivity, which can be written in the form

$$R=\frac{\eta}{Z_A}\frac{4a^2e^2}{\hbar^2\varepsilon_0^2}\frac{I_p}{A^2}\frac{1}{\omega^4|\varepsilon(\omega)|^2} \tag{1}$$

is proportional to I_p and to A^{-2} and the frequency dependence is given by $\omega^{-4}|\varepsilon(\omega)|^{-2}$. For simplicity, we use the dielectric function $\varepsilon=(d_1\varepsilon_{\mathrm{GaAs}}+d_2\varepsilon_{\mathrm{AlAs}})/a$, where d_1 and d_2 are the thicknesses of the GaAs and AlAs layers, respectively, and $\varepsilon_{\mathrm{GaAs}}$ and $\varepsilon_{\mathrm{AlAs}}$ are the dielectric functions of the bulk materials, which we describe by Lorentzian curves with $\nu_{\mathrm{TO}}=8.0\,\mathrm{THz}$, $\varepsilon(0)=12.9$, $\varepsilon(\infty)=10.9$ for GaAs, and $\nu_{\mathrm{TO}}=10.8\,\mathrm{THz}$, $\varepsilon(0)=10.06$, $\varepsilon(\infty)=8.16$ for AlAs.[5] The calculated responsivity (Fig. 2, solid line) delivers a damping constant (0.45 THz) which is larger by a factor of 6 then the damping constant of bulk GaAs;[6] we suggest that roughness of the GaAs/AlAs interfaces caused a broadening of the phonon resonances. For the coupling between radiation and antenna we found that the efficiencies ($\eta=2\times10^{-3}$ for detector A and 10^{-2} for detector B) were small, most likely because of nonperfect adjustment of the antenna wire or due to the finite wire thickness. We suppose that the intraminiband relaxation was mainly determined by inelastic scattering; in an inelastic scattering process an electron looses energy to phonons. However, elastic scattering especially due to interface roughness can diminish the direct current[7,8] and also the modulation degree.

We finally discuss the possibility of an ideal superlattice detector (for a frequency ω), which has a perfect matching between the antenna and the free space on the one side and the superlattice on the other side. For the ideal detector the real parts of the antenna conductance and of the electron–superlattice conductance are equal and the imaginary part of the antenna conductance is equal to the sum of the imaginary parts of the dielectric and electron–superlattice conductances; now, the real part of the dielectric conductance has to be small compared to the real part of the electron conductance, i.e., the THz current through the superlattice is mainly carried by the electrons. A detailed analysis using the equivalent circuit, [Fig. 1(c)] delivers[9] the responsivity of the ideal detector (for $\omega_B\tau=1$) $R_{id}=e\tau(2N\hbar)^{-1}=(\omega\tau/2N)e(\hbar\omega)^{-1}$, where N is the number of superlattice periods ($Na=L$). The ideal responsivity is thus equal to the product of the quantum limit $e(\hbar\omega)^{-1}$ of detection and the quality factor $\omega\tau$, which is a measure of the number of oscillations of an electron in the THz field within the lifetime τ, divided by twice the number of superlattice periods.

In Fig. 3 we have drawn, besides the experimental points and the theoretical curves for the superlattices A and B, the responsivity of the ideal superlattice detector, which lies by an order of magnitude below the quantum limit and, additionally, a theoretical responsivity R^* for a superlattice of type B, but with a diameter of 1 μm (rather than 5 μm in our experiment), assuming $\eta=0.2$ and phonon damping ($\gamma=0.07\,\mathrm{THz}$) as in bulk crystals. We suggest that R^* may be attainable for a superlattice of high quality of the interfaces and an antenna with a wire (diameter 10 μm rather than 25 μm as in our experiment) having a negligible inductance.

Our experimental results together with the analysis indicate that the superlattice detector has a wide range of response. We expect that the upper frequency limit is determined by the miniband width, which corresponds to about 30 THz for superlattice B. By designing superlattices with still larger miniband width, the upper limit can be further extended. Phonon resonances, which diminish the responsivity, can be shifted by choosing other superlattice materials.

In conclusion, we have shown that the superlattice detector, based on Bloch oscillations of miniband electrons, is suitable for detection of THz radiation in a wide frequency range, with a responsivity having minima at the frequencies of infrared active phonons.

The research was supported by the Deutsche Forschungsgemeinschaft. The authors acknowledge support by the Stiching voor Fundamental Onderzoeg der Materie (FOM) in providing beam time on FELIX and appreciate the assistance of the FELIX staff.

[1] A. A. Ignatov, E. Schomburg, K. F. Renk, W. Schatz, J. F. Palmier, and F. Mollot, Ann. Phys. **3**, 137 (1994).
[2] S. Winnerl, E. Schomburg, J. Grenzer, H.-J. Regl, A. A. Ignatov, A. D. Semenov, K. F. Renk, D. G. Pavel'ev, Yu. Koschurinov, B. Melzer, V. Ustinov, S. Ivanov, S. Schaposchnikov, and P. S. Kop'ev, Phys. Rev. B **56**, 10303 (1997).
[3] S. Winnerl, W. Seiwerth, E. Schomburg, J. Grenzer, K. F. Renk, C. J. G. M. Langerak, A. F. G. van der Meer, D. G. Pavel'ev, Yu. Koschurinov, A. A. Ignatov, B. Melzer, V. Ustinov, S. Ivanov, and P. S. Kop'ev, Appl. Phys. Lett. **73**, 2983 (1998).
[4] L. Esaki and R. Tsu, IBM J. Res. Dev. **14**, 61 (1970).
[5] *Landolt-Börnstein*, edited by O. Madelung, M. Schulz, and H. Weiss (Springer, New York, 1982), Vol. 17a.
[6] *Properties of Gallium Arsenid* (INSPEC, New York, 1986).
[7] E. Schomburg, M. Henini, J. M. Chamberlain, D. P. Steenson, S. Brandl, K. Hofbeck, K. F. Renk, and W. Wegscheider, Appl. Phys. Lett. **74**, 2179 (1999).
[8] E. Schomburg, T. Blomeier, K. Hofbeck, J. Grenzer, S. Brandl, I. Lingott, A. A. Ignatov, K. F. Renk, D. G. Pavel'ev, Yu. Koschurinov, B. Ya. Melzer, V. Ustinov, S. Ivanov, A. Zhukov, and P. S. Kop'ev, Phys. Rev. B **58**, 4035 (1998).
[9] A. A. Ignatov and A.-P. Jauho, J. Appl. Phys. **85**, 3643 (1999).